REVISTA DE METALURGIA, vol. 46
NÚMERO EXTRAORDINARIO, 133-137, 2010
ISSN: 0034-8570
eISSN: 1988-4222
doi: 10.3989/revmetalmadrid.16XIIPMS

Continuum modeling of $\{10\bar{1}2\}$ twinning in a Mg-3%Al-1%Zn rolled sheet

A. Jérusalem*, A. Fernández* and M.T. Pérez-Prado*

Abstract A crystal plasticity continuum model with differentiated self- and cross- hardening mechanisms for twin and slip systems has been utilized to predict the slip/twin activities and texture evolution in a rolled and annealed Mg-3%Al-1%Zn sheet compressed along the rolling direction (RD) and tensile tested along the normal direction (ND). The contribution of twinning is significantly larger during tension along ND, leading to a significant texture change with strain. A good correlation is found between simulations and recent experimental results.

Keywords Magnesium alloys; Twinning; Continuum modeling; Crystal plasticity.

Modelización del maclado $\{10\bar{1}2\}$ de una chapa laminada de Mg-3%Al-1%Zn

Resumen Un modelo continuo de plasticidad cristalina, que contempla los mecanismos de auto-endurecimiento y endurecimiento cruzado para los sistemas de maclado y deslizamiento, se ha utilizado para predecir las actividades de deslizamiento y del maclado, así como la evolución de la textura, de una chapa laminada y recocida de la aleación de magnesio Mg-3%Al-1%Zn ensayada en compresión, a lo largo de la dirección de laminación (DL) y en tensión, a lo largo de la dirección normal (DN). Se encontró que la contribución del maclado es mucho más importante cuando la muestra se tensiona a lo lago de DN, lo que da lugar a un cambio fuerte de textura. Se observó una buena correspondencia entre las simulaciones y resultados experimentales recientes.

Palabras clave Aleaciones de magnesio; Maclado; Modelización continua; Plasticidad cristalina.

1. INTRODUCTION

The potential of lightweight magnesium alloys to replace heavier materials in transportation vessels is now clearly established[1 and 2]. Many efforts have been devoted over the last decade to understand the behavior of these materials and the main mechanisms governing the plasticity of commercial alloys are quite well understood[3-34]. It is now widely accepted that, at room temperature and low strain rates, Mg alloys with a random texture deform mainly by basal slip and $\{10\bar{1}2\}$ twinning. In strongly textured alloys, such as those resulting from rolling and extrusion processes, the operative deformation mechanisms are highly dependent on the relative orientation between the applied stress and the c-axis[3-34].

In particular, $\{10\bar{1}2\}$ twinning is only activated when the application of an external load leads to an extension of the lattice along the c-axis. It is therefore called "extension twinning" [26]. In a rolled and annealed AZ31 sheet, with a strong {0001} texture, the so-called c-axis extension can be caused either by uniaxial tension along the c-axis or by uniaxial compression along a direction perpendicular to the c-axis. It has been recently demonstrated experimentally[34] that the $\{10\bar{1}2\}$ twinning characteristics, such as active twin variants, twin morphology, volume fraction of twins with strain and twin texture, are significantly dependent on the strain path. Specifically, when a compressive load is applied perpendicular to the c-axis, one or two twin variants are activated, whereas all six variants become active when a tensile load is applied parallel to the c-axis, leading to significant differences in the flow stress, in the relative twin and slip activities, and in the strain hardening behavior.

Developing models that can predict the evolution of the microstructure as well as the mechanical behavior of magnesium alloys is now timely. Despite the availability of other simulation techniques, such

* IMDEA Materials Institute, Calle Profesor Aranguren, s/n, 28040 Madrid, Spain.

as dislocation dynamics[35 and 36] or atomistic simulations [37 and 38], finite element method (FEM) is one of the techniques that describes best crystal deformation mechanisms while avoiding the drastic length- and time-scale limitations of the other two. Recently, Fernandez *et al.*[39] complemented a model by Staroselski and Anand[40], adding differentiated self- and cross-hardening between slip and twin systems, and taking a special attention to the individual calibration of each one of the interaction parameters. The validity of this model to simulate the texture evolution and the stress-strain curves of a Mg AZ31 rolled sheet deformed at room temperature and quasi-static strain rate in uniaxial compression along the rolling (RD) and normal (ND) directions was demonstrated[39].

The aim of this paper is to apply the continuum model by Fernandez *et al.*[39] to simulate the activity of the different deformation mechanisms and the deformation texture in a rolled AZ31 alloy subjected to uniaxial tension along the normal direction, ND, (*i.e.*, parallel to the c-axis) and uniaxial compression along the rolling direction, RD (*i.e.*, in a direction perpendicular to the c-axis). Special emphasis is placed in analyzing the $\{10\bar{1}2\}$ twinning activity in both cases. The results are compared to experimental data reported recently[34]. Tensile deformation of Mg alloys along the c-axis was so far not investigated, as it was not practically viable to extend a strongly textured rolled sheet along its ND. However, this deformation path has recently become of great interest as novel alloys with rare earth additions are being developed, whose rolling textures are either much weaker than those of commercial alloys and/or tilted away from them[41].

2. SIMULATION METHODOLOGY

The general crystal plasticity constitutive framework of the continuum model used here[39] includes all slip and twin systems of HCP crystals, as well as the polarity condition of tensile twinning. The model parameters, including the ones associated to the added cross-hardening formulation, were carefully calibrated and validated against uniaxial compression experiments in[39]. Here, an idealized polycrystalline mesh of 2,592 cubic elements (each one representing an individual grain), was subjected to uniaxial compression along RD and tension along ND. Figure 1 illustrates the starting texture, chosen to match approximately the experimental texture reported in[34]. This texture is formed by an isotropic (0001) fiber, with a spread of approximately 15°, as is characteristic of rolled and annealed Mg alloys.

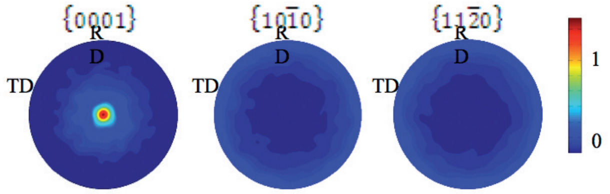

Figure 1. Initial texture of the AZ31 sheet used in the simulations.

Figura 1. Textura inicial de la chapa AZ31 utilizada en las simulaciones.

Simulations were carried out complying with conventional experimental boundary conditions and up to a strain of 16 %, at which rolled Mg AZ31 is reported to fail when tested under the conditions investigated here[34].

3. RESULTS AND DISCUSSION

Figure 2 depicts the predicted normalized $\{10\bar{1}2\}$ twinning and slip activities during a compression test along RD (Fig. 2 a)), as well as the simulated {0001},

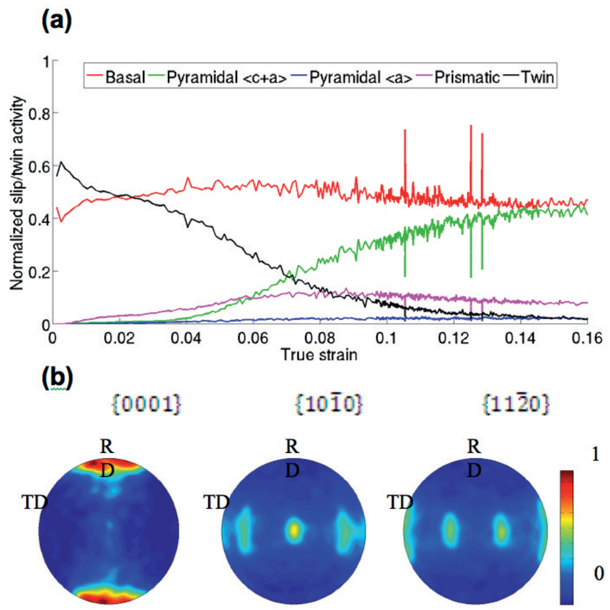

Figure 2. (a) Slip/twin activities during uniaxial compression along RD; (b) Texture simulated for a strain of 15 %.

Figura 2. (a) Actividades del deslizamiento y el maclado durante la compresión a lo largo de la dirección de laminación; (b) Textura simulada para una deformación del 15 %.

 Rev. metal. Madrid, 46 (Número Extraordinario), 133-137, 2010, ISSN: 0034-8570, eISSN: 1988-4222, doi: 10.3989/revmetalmadrid.16XIIPMS

$\{10\bar{1}0\}$, and $\{11\bar{2}0\}$ pole figures corresponding to a strain of 15 % (Fig. 2 b)). Note that the observed oscillations are due to small numerical instabilities related to the explicit scheme. Temporal convergence has been checked and these spurious modes have been shown to have no influence on the overall activity. It can be seen in figure 2 a) that, during compression along RD, twinning predominates at the early deformation stages (up to approximately 3 %) and at higher strains its activity decreases gradually until it becomes inactive at approximately 12 % deformation. Basal slip operates in combination with $\{10\bar{1}2\}$ twinning from the onset of deformation, and its activity increases gradually until it saturates at around 0.5 at a strain of 5 %. It continues to have approximately the same activity level until failure. It is well known that twinning causes a lattice rotation of 86.3° and therefore in the rotated grains the compression stress is being applied parallel to the ND in most grains. At that point extension twinning and prismatic slip are severely hindered and, thus, pyramidal <c+a> slip becomes increasingly active. We observe the onset of pyramidal <c+a> slip at a strain of 4 %, at which others have also reported the presence of a significantly large fraction of twinned grains[42]. During the last deformation stages the strain is mainly accommodated by basal and pyramidal <c+a> slip, with minor contributions of prismatic and pyramidal <a> slip. The operation of <c+a> pyramidal slip during compression along RD at room temperature has been reported previously in several works[43]. Figure 2 b) illustrates how, as a consequence of twinning, basal poles become almost perpendicular to ND and are confined within ±30° of RD (rotation angle toward TD).

Figure 3 shows the predicted normalized $\{10\bar{1}2\}$ twinning and slip activities corresponding to the tension test along ND (Fig. 3 a)) as well as the simulated $\{0001\}$, $\{10\bar{1}0\}$, $\{11\bar{2}0\}$ and pole figures corresponding to a strain of 15 % (Fig. 3 b)). Significant differences can be noticed with respect to the case described above (compression along RD). Most importantly, $\{11\bar{2}0\}$ twinning plays a more prominent role during deformation, being active almost until failure (16 %). Basal slip is also activated from the onset of deformation, and its activity is practically constant at all strains (and approximately equal to 0.5). Again, twinning causes a lattice rotation of 86.3º, and in the rotated grains the tensile stress is applied approximately perpendicular to the c-axis. At this point, both prismatic and pyramidal <a> and <c+a> slip systems are favourably oriented for slip, but prismatic is activated preferentially, presumably due to its lower CRSS [44]. The activation of prismatic slip starts approximately at a strain of 1 %. Pyramidal

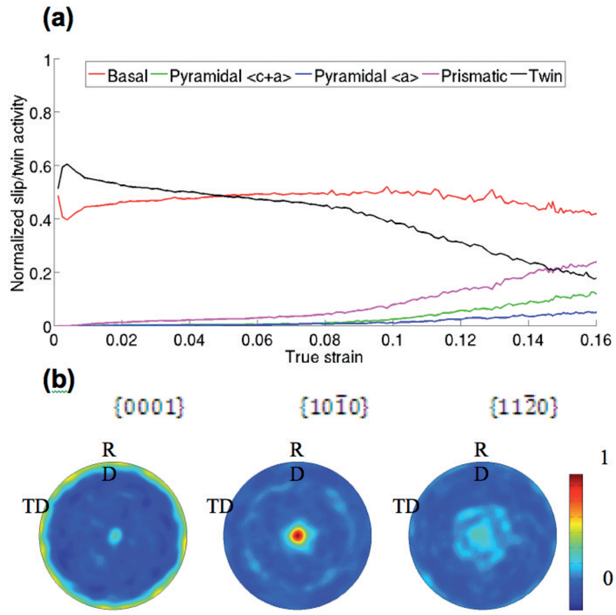

Figure 3. (a) Slip/twin activities during uniaxial tension along ND; (b) Texture simulated for a strain of 15%.

Figura 3. (a) Actividades del deslizamiento y el maclado durante un ensayo de tensión uniaxial a lo largo de la dirección normal; (b) Textura simulada para una deformación del 15%.

systems are activated at a strain of 5 %. Figure 3 b) shows that the basal poles are now widely spread along the RD-TD plane.

We now compare the predictions of the model by Fernandez *et al.*[39] shown above with the experimental results reported recently by Hong *et al.*[34]. Both simulations and experiments reveal that the contribution of twinning to the deformation of the AZ31 rolled sheet is dependent on the strain path. In particular, it is significantly higher when testing is carried out under tension along ND than under compression along RD. In compression, a transition from twin- to slip-dominated deformation was observed experimentally at a strain of 6% and by simulation at 3 %. In tension, Hong *et al.*[34] suggest that a transition from slip- to twin- and then, again, to slip-dominated flow takes place with increasing strain. They estimate the predominant deformation mechanism by measuring the volume fraction of twins with strain. In particular, they suggest that, at a strain of 1 %, the contribution of twinning is only 10 %. Simulations, however, reveal a predominance of twinning during the first stages of tensile deformation (up to ~4 %). The differences between the slip/twin activities estimated experimentally and by simulations might be attributed to several factors. First, in the experimental report[34] the twin volume fraction was estimated by adding twinned areas along several cross sections, whereas the model carries out these estimations in the bulk. It cannot be ruled out that some relaxation of the structure might take place during sectioning. And secondly, the initial simulated and experimental textures are similar, but since the CRSS of basal slip is very low[44], even very small differences in the initial texture might result in significant variations of the slip/twin activities at the early stages of deformation.

The experimental and simulated textures illustrate that the operation of {11$\bar{2}$0} twinning during the compression test leads to the concentration of the basal poles in a plane perpendicular to ND, at approximately ±30° of RD toward TD. This confinement is attributed to the operation of just one twin variant pair in most grains[35], as is *a priori* expected from the preference of shear zone formation under compression as opposed to tension. During tension, both simulation and experiments show that twinning leads to a wider spread of the basal poles in the RD-TD plane, which is caused by the operation of multiple twin variants[34]. If all six twin variants are equally active, which would be the case when the starting texture is a perfect fiber (*i.e.*, when the c-axis in all grains is perfectly aligned with ND), then a random distribution of basal poles in the RD-TD plane would result. Otherwise some deviations from this ideal texture occur, as not all six twin variants have equal contributions, and therefore several intensity maxima can be observed in the outer ring of the {0001} pole figure (Fig. 3 b)). A very good correlation exists between the experimental and simulated textures. Similarly, it can be expected that, if the same AZ31 sample was deformed by plane strain, i.e., compressing along ND and restricting plastic deformation along, for example, TD, the number of twin variants activated would be higher than in the current ND compression test but lower than in tension along ND. This modelling effort, thus, helps to predict the texture evolution in this Mg alloy under other strain paths than those contemplated here.

4. SUMMARY

In summary, the continuum model developed recently by Fernández *et al.*[39] based on a previous model by Staroselsky and Anand[40] is used to predict the slip and twin activities as well as the deformation texture evolution during uniaxial compression along RD and tension along ND in a rolled and annealed Mg AZ31 sheet. A good correlation is found between predictions and experiments. This model might, therefore, be applicable to correctly predict the deformation behavior of recently developed wrought Mg alloys with weaker textures or with textures tilted away from the conventional <0001> (rolling) and <10-10> (extrusion) fibers. These novel alloys are particularly attractive because of their more isotropic yield stress behaviour[41 and 45] and excellent ductilities.

Acknowledgements

A.J. acknowledges support from the Juan de la Cierva grant from the Spanish Ministry of Science and Innovation and from the AMAROUT – FP7 Marie Curie Action People COFUND Programme grant from the European Union. The authors would like to thank the vehicle interior manufacturer, Grupo Antolin Ingenieria, S.A., within the framework of the project MAGNO2008-1028-CENIT Project funded by the Spanish Ministry as well as the ESTRUMAT-S2009/MAT-1585 grant (Madrid Regional Government). They are finally grateful to Prof. Lallit Anand at the Massachusetts Institute of Technology for supplying for their research the original Abaqus/Explicit VUMAT subroutine for rate-independent crystal plasticity for HCP materials written by Staroselsky and Anand[40], and modified by Fernandez *et al.*[39].

REFERENCES

[1] M. Bamberger and G. Dehm, *Ann. Rev. Mater. Res.* 38 (2008) 505-533.

[2] M. Easton, A. Beer, M. Barnett, C. Davies, G. Dunlop, Y. Durandet, S. Blacket, T. Hilditch and P. Beggs, *JOM* 60 (2008) 57-62.

[3] S.L. Couling, J.F. Pashak and L. Sturkey, *Trans. ASM* 51 (1959) 94-107.

[4] U.F. Kocks and D.G. Westlake, *Trans. AIME* 239 (1967) 1107-1109.

[5] E.W. Kelley and W.F. Hosford, *Trans. AIME* 242 (1968) 654-660.

[6] A. Couret and D. Caillard, *Acta Metall.* 33 (1985) 1455-1462.

[7] G.Y. Chin and W.L. Mammel, *Metall. Trans.* 1 (1970) 357-361.

[8] M.H. Yoo, *Metall. Trans.* 12A (1981) 409-418.

[9] S.S. Vagarali and T.G. Langdon, *Acta Metall.* 29 (1981) 1969-1982.

[10] M.G. Zelin, H.S. Yang, R.Z. Valiev and A.K. Mukherjee, *Metall. Trans.* 23 (1992) 3135-3140.

[11] N. Munroe and X. Tan, *Scr. Mater.* 36 (1997) 1383-1386.
[12] S.R. Agnew, M.H. Yoo and C.N. Tomé, *Acta Mater.* 49 (2001) 4277-4289.
[13] H. Watanabe, H. Tsutsui, T. Mukai, M. Kohzu, S. Tanabe and K. Higashi, *Int. J. Plasticity* 17 (2001) 387-397.
[14] M.R. Barnett, *J. Light Metals* 1 (2001) 167-177.
[15] S.R. Agnew, C.N. Tomé, D.W. Brown, T.M. Holden and S.C. Vogel. *Scr. Mater.* 48 (2003) 1003-1008.
[16] A. Galiyev, O. Sitdikov and R. Kaibyshev, *Mater. Trans.* 44 (2003) 426-431.
[17] J. Koike, T. Kobayashi, T. Mukai, H. Watanabe, M. Suzuki, K. Maruyama and K. Higashi, *Acta. Mater.* 51 (2003) 2055-2065.
[18] M.R. Barnett, *Metall. Mater. Trans.* 34 (2003) 1799-1806.
[19] R. Gehrmann, M.M. Frommert and G. Gottstein, *Mater. Sci. Eng.* 395 (2005) 338-349.
[20] M.R. Barnett, Z. Keshavarz, A.G. Beer and D. Atwell, *Acta Mater.* 52 (2004) 5093-5103.
[21] S.R. Agnew and Ö. Duygulu, *Int. J. Plasticity* 21 (2005) 1161-1193.
[22] J.A. del Valle, M.T. Pérez-Prado and O.A. Ruano. *Metall. Mater. Trans.* 36 (2005) 1427.
[23] Z. Keshavarz and M.R. Barnett, *Scr. Mater.* 55 (2006) 915-918.
[24] E. Meza-García, P. Dobroň, J. Bohlen, D. Letzig, F. Chmelik, P. Lukáč and K.U. Kainer, *Mater. Sci. Eng.* 462 (2007) 297-301.
[25] M.R. Barnett, *Mater. Sci. Eng.* 464 (2007) 1.
[26] J.A. Del Valle and O.A. Ruano, *Acta Mater.* 55 (2007) 455-466.
[27] T. Al-Samman and G. Gottstein, *Mater. Sci. Eng.* 488 (2008) 406-414.
[28] Y. Chino, K. Kimura and M. Mabuchi, *Mater. Sci. Eng.* 486 (2008) 481-488.
[29] A. Jain, Ö. Duygulu, D.W. Brown, C.N. Tomé and S.R. Agnew, *Mater. Sci. Eng.* 486 (2008) 545-555.
[30] B. Hutchinson, M.R. Barnett, A. Ghaderi, P. Cizek and I. Sabirov, *Int. J. Mat. Res.* 100 (2009) 556-563.
[31] E.A. Ball and P.B. Prangnell, *Scr. Metall. Mater.* 31 (1994) 111-116.
[32] X.Y. Lou, M. Li, R.K. Boger, S.R. Agnew and R.H. Wagoner, *Int. J. Plasticity* 23 (2007) 44-86.
[33] S. Yi, Y. Shestakow and S. Zaefferer, *Mater. Sci. Eng.* 516 (2009) 58-64.
[34] S.G. Hong, S.H. Park and C.S. Lee, *Acta Mater.* 58 (2010) 5873-5885.
[35] H.N. Zbib, M. Rhee and J.P. Hirth, *Int. J. Mech. Sci.* 40 (1998) 113-127.
[36] J. Segurado, J. Llorca and I. Romero, *Mod. Sim. Mat. Sci. Eng.* 15 (2007) S361-S375.
[37] J. Wang, J.P. Hirth and C.N. Tomé, *Acta Mater.* 57 (2009) 5521-5530.
[38] L. Yue, H. Zhang and D.Y. Li, *Acta Mater.* 58 (2010) 2677-2684.
[39] A. Fernández, M.T. Pérez-Prado, Y. Wei and A. Jérusalem, *Int. J. Plasticity* (2010), submitted.
[40] A. Staroselsky and L. Anand, *Int. J. Plasticity* 19 (2003) 1843-1864.
[41] J. Bohlen, S. Yi, D. Letzig and K.U. Kainer, *Mater. Sci. Eng.* A 527 (2010) 7092-7098.
[42] J. Jiang, A. Godfrey, W. Liu and Q. Liu, *Mater. Sci. Eng.* A 483-484 (2008) 576-579.
[43] S.B. Yi, C.H.J. Davies, H.G. Brokmeier, R.E. Bolmaro, K.U. Kainer and J. Homeyer, *Acta Mater.* 54 (2006) 549-562.
[44] B. Clausen, C.N. Tomé, D.W. Brown and S.R. Agnew, *Acta Mater.* 56 (2008) 2456-2468.
[45] N. Stanford and M.R. Barnett, *Mater. Sci. Eng.* 496 (2008) 399-408.